Supplemental digital content

Single-nucleus atlas of sevoflurane-induced hippocampal cell-type- and sex-specific effects during development in mice

Shao-yong Song, Ke Peng, Xiao-wen Meng, Xi-sheng Shan, Qing-cai Chen, Wei-ming Zhao, Biyu Shen, Hong Qiu, Hong Liu, Hua-yue Liu, Fu-hai Ji

Supplemental Figure 1.

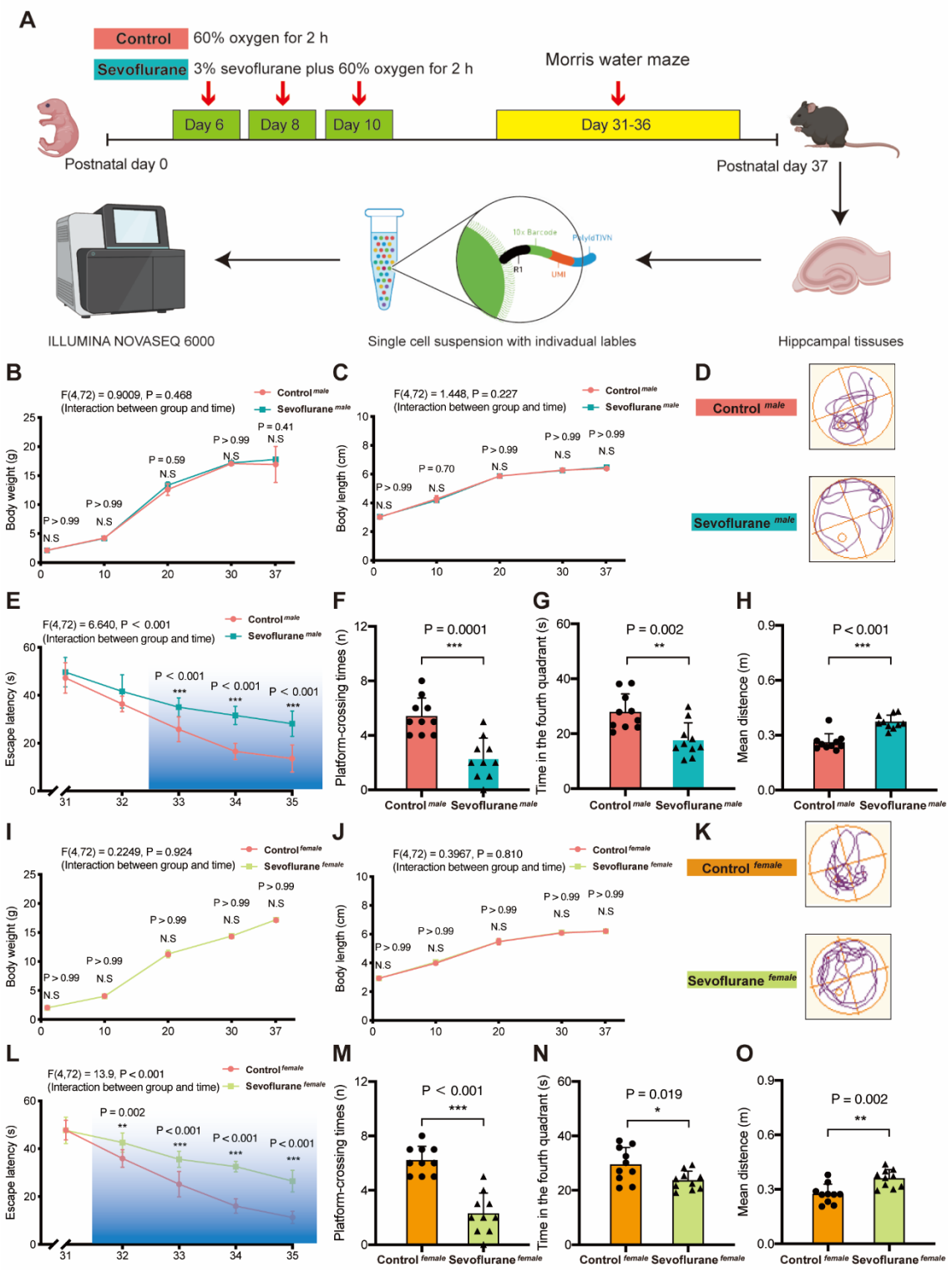

Supplemental Figure 1. Morris water maze behavior tests of male and female mice

(A) Schematic diagram: 3% sevoflurane or control treatment for 2 h on postnatal day 6, 8, and 10, Morris water maze tests on postnatal day 31–36, and single-nucleus RNA sequencing of hippocampus on postnatal day 37. **(B)** Body weight of male mice on postnatal day 1, 10, 20, 30, and 37. **(C)** Body length of male mice on postnatal day 1, 10, 20, 30, and 37. **(D)** Trace plots of male mice on postnatal day 36. **(E)** Escape latency of male mice on postnatal day 31–35. **(F)** Platform-crossing times of male

mice on postnatal day 36. **(G)** Time spent in the fourth quadrant of male mice on postnatal day 36. **(H)** Mean distance from the platform of male mice on postnatal day 36. **(I)** Body weight of female mice on postnatal day 1, 10, 20, 30, and 37. **(J)** Body length of female mice on postnatal day 1, 10, 20, 30, and 37. **(K)** Trace plots of female mice on postnatal day 36. **(L)** Escape latency of female mice on postnatal day 31–35. **(M)** Platform-crossing times of female mice on postnatal day 36. **(N)** Time spent in the fourth quadrant of female mice on postnatal day 36. **(O)** Mean distance from the platform of female mice on postnatal day 36. Data are means ± SD. n = 10 mice/group. Student's t-test or two-way repeated measures ANOVA with Bonferroni correction. **P < 0.01, ***P < 0.001.

Supplemental Figure 2.

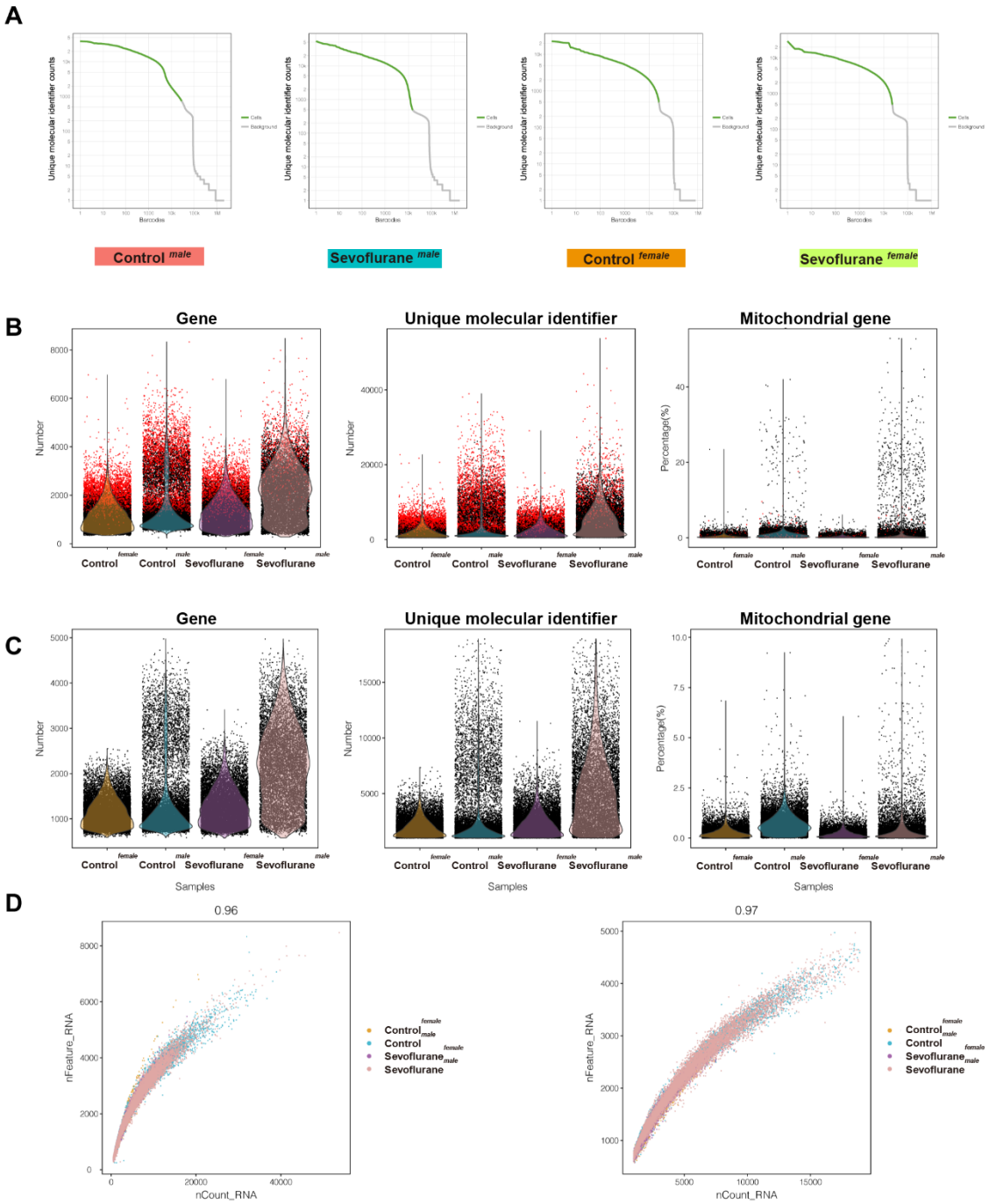

Supplemental Figure 2. Single-nucleus RNA sequencing quality control

(A) Estimated cells (green) and background (grey) in the control ^{male}, sevoflurane ^{male}, control ^{female}, and sevoflurane ^{female} groups using the Cell Ranger software. **(B)** Distribution of genes, unique molecular identifier, and mitochondrial genes before filtering in the 4 groups. **(C)** Distribution of genes, unique molecular identifier, and mitochondrial genes after filtering in the 4 groups. **(D)** Correlation between the number of unique molecular identifier and the number of genes before filtering (left) and after filtering (right).

Supplemental Figure 3.

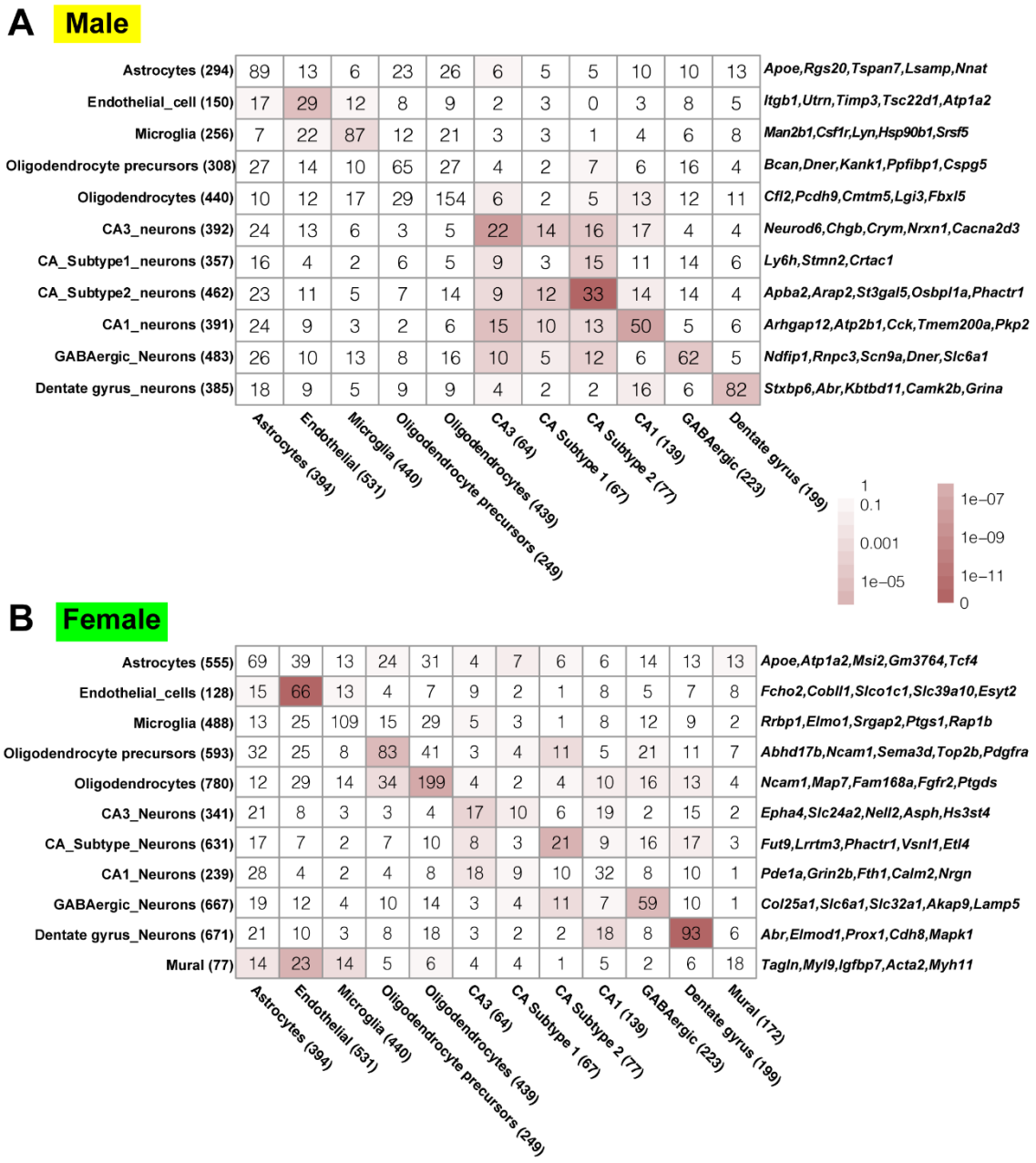

Supplemental Figure 3. Overlap of cluster-specific gene signatures with the previously defined hippocampal cell types markers

(A) Male mice. **(B)** Female mice. Cluster-specific gene numbers are indicated in the parenthesis. Enrichment was assessed using Fisher's exact test with Bonferroni adjusted p values. Color intensity indicates statistical significance of overlapping genes, and the numbers of overlapping cluster-specific genes between our cluster-specific gene and previously known markers are shown in the cells. Top cell marker genes determined by our single-nucleus RNA sequencing data are listed on the right of the plot.

Supplemental Figure 4.

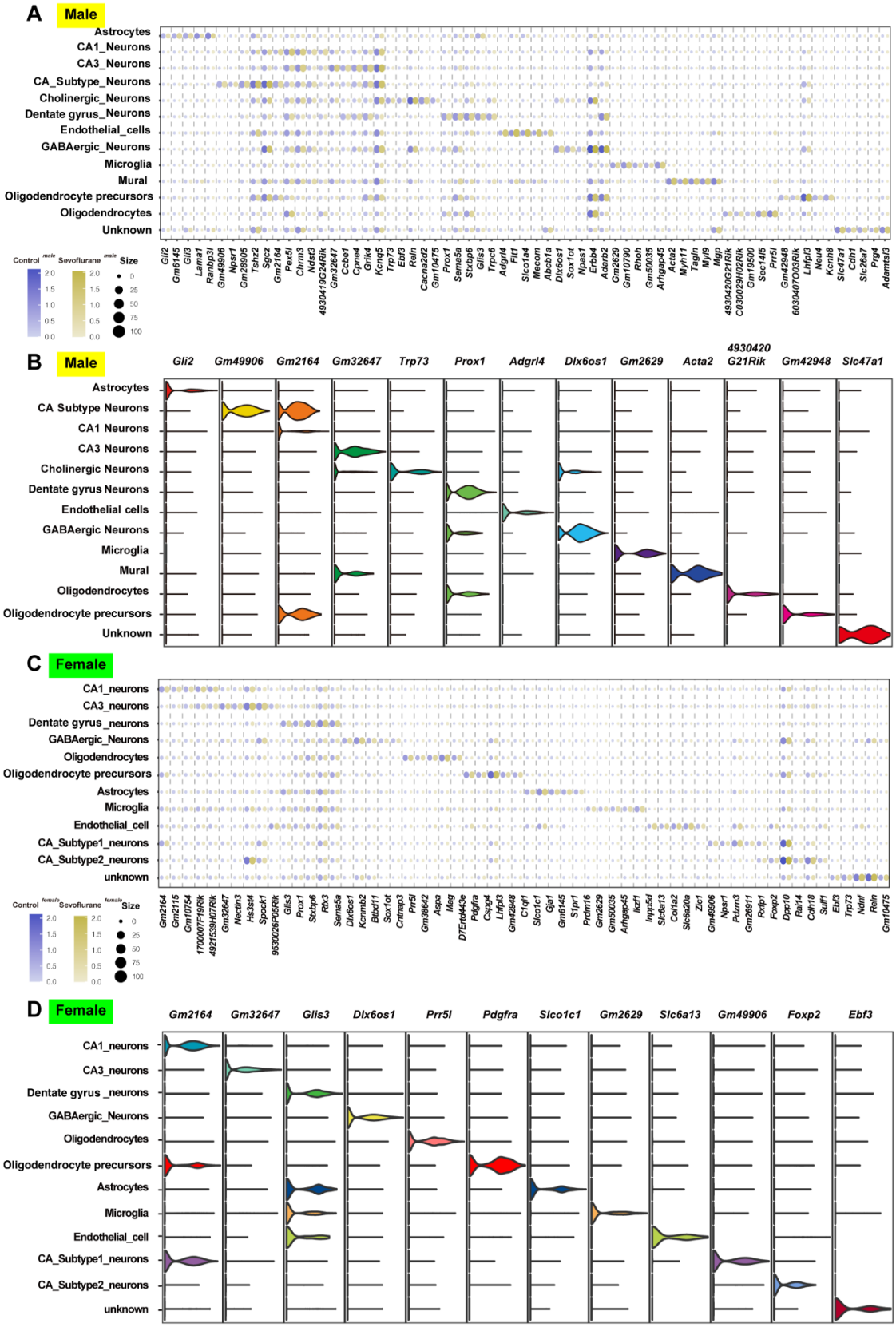

Supplemental Figure 4. Identification and cross-validation of novel cell type-specific marker genes in male and female mice

(A) Dot plot showing the expression of top 5 genes for each specific hippocampal cell type of male mice. Dot size is proportional to the fraction of cells expressing specific genes, and color intensity corresponds to the level of gene expression. **(B)** Violin plot showing the normalized expression of top cell type-specific marker genes (columns) in specific cell types (rows) of male mice. **(C)** Dot plot showing the expression of top 5 genes for each specific hippocampal cell type of female mice. Dot size is proportional to the fraction of cells expressing specific genes, and color intensity corresponds to the level of gene expression. **(D)** Violin plot showing the normalized expression of top cell type-specific marker genes (columns) in specific cell types (rows) of female mice. Criteria for specific marker genes: mincell_pct ≥ 0.25, P value ≤ 0.01, and $\log_2$ (fold change) ≥ 0.361 (Seurat R package).

Supplemental Figure 5.

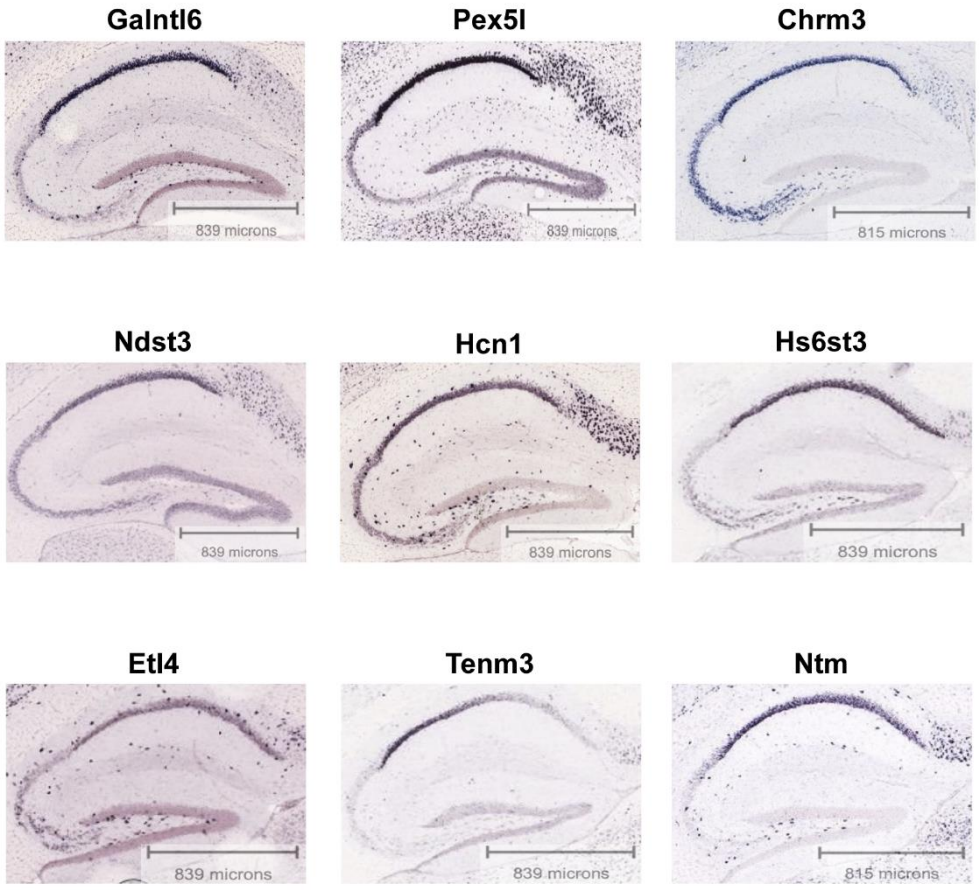

Supplemental Figure 5. Validation of CA1 neuron-specific marker genes

The top marker genes for CA1 neurons identified by our single cell sequencing approach were validated using the in-situ hybridization images in the Allen Brain Atlas (https://mouse.brain-map.org).

Supplemental Figure 6.

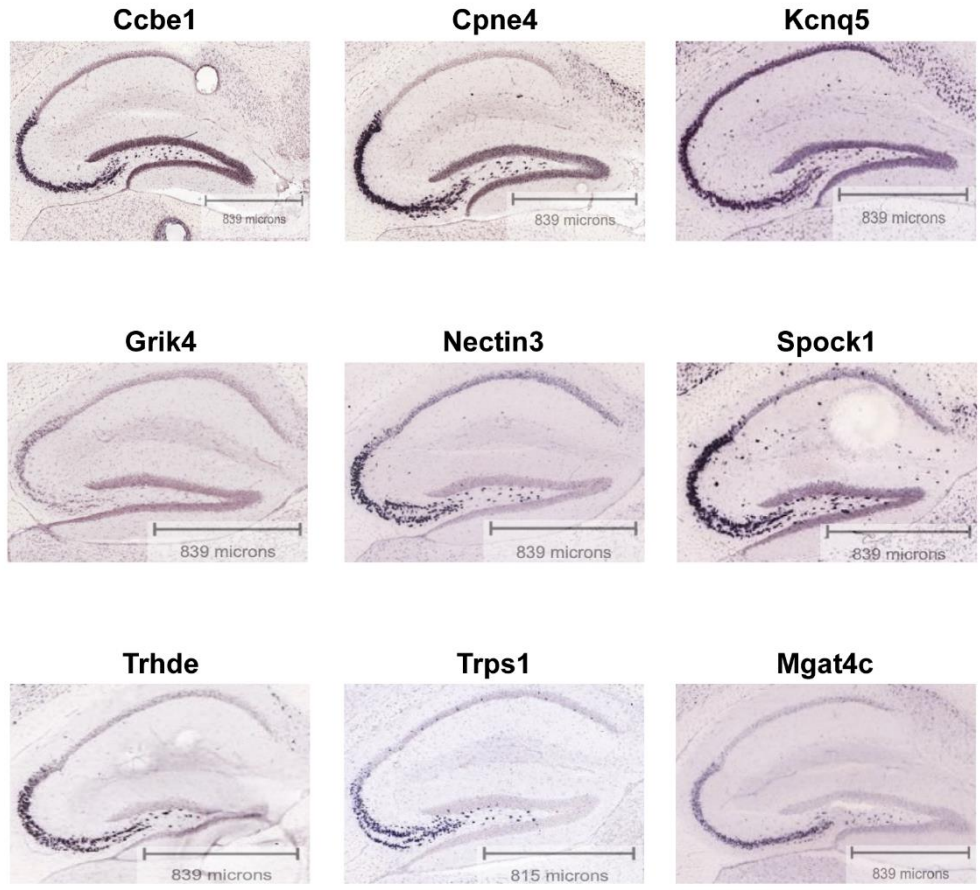

Supplemental Figure 6. Validation of CA3 neuron-specific marker genes

The top marker genes for CA3 neurons identified by our single cell sequencing approach were validated using the in-situ hybridization images in the Allen Brain Atlas (https://mouse.brain-map.org).

Supplemental Figure 7.

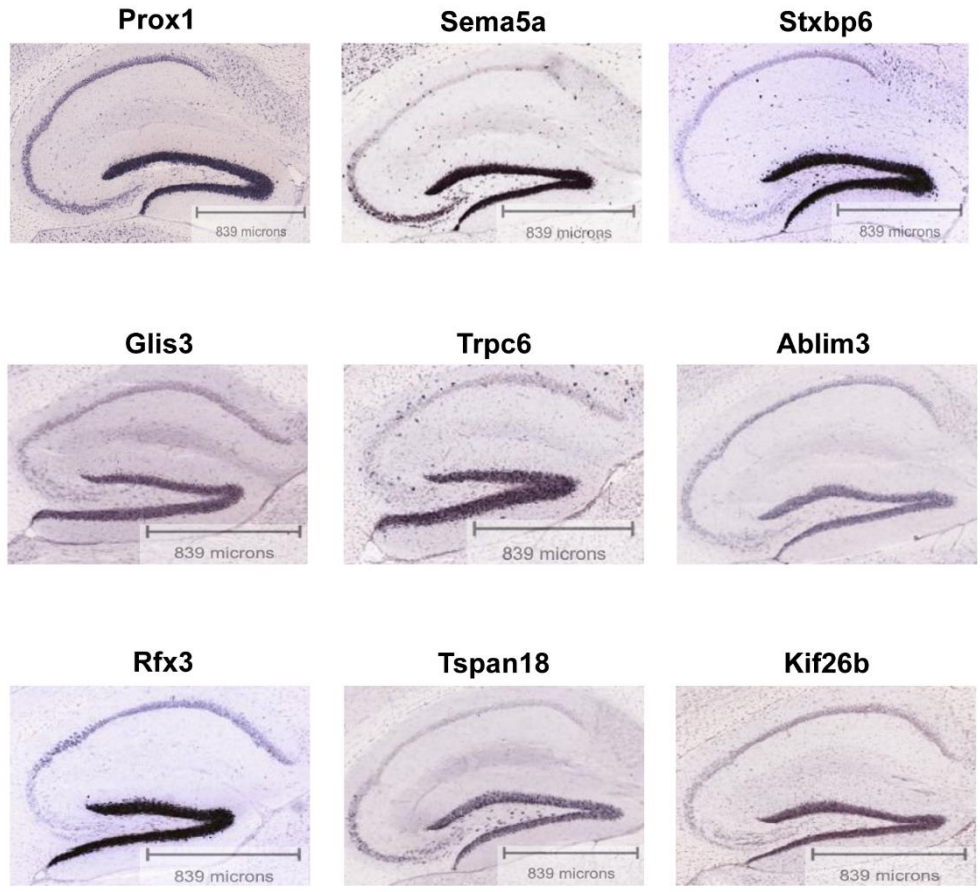

Supplemental Figure 7. Validation of dentate gyrus granule cell-specific marker genes

The top marker genes for dentate gyrus granule cells identified by our single cell sequencing approach were validated using the in-situ hybridization images in the Allen Brain Atlas (https://mouse.brain-map.org).

Supplemental Figure 8.

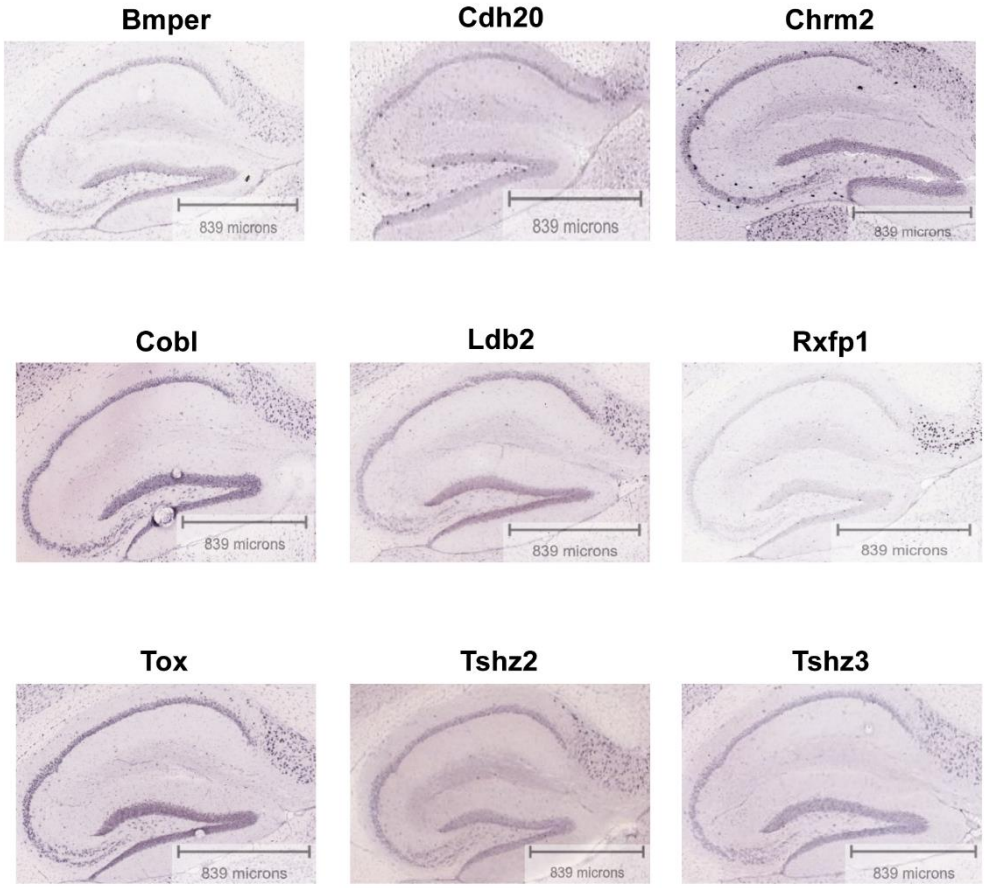

Supplemental Figure 8. Validation of CA subtype neuron-specific marker genes

The top marker genes for CA subtype neurons identified by our single cell sequencing approach were validated using the in-situ hybridization images in the Allen Brain Atlas (https://mouse.brain-map.org).

Supplemental Figure 9.

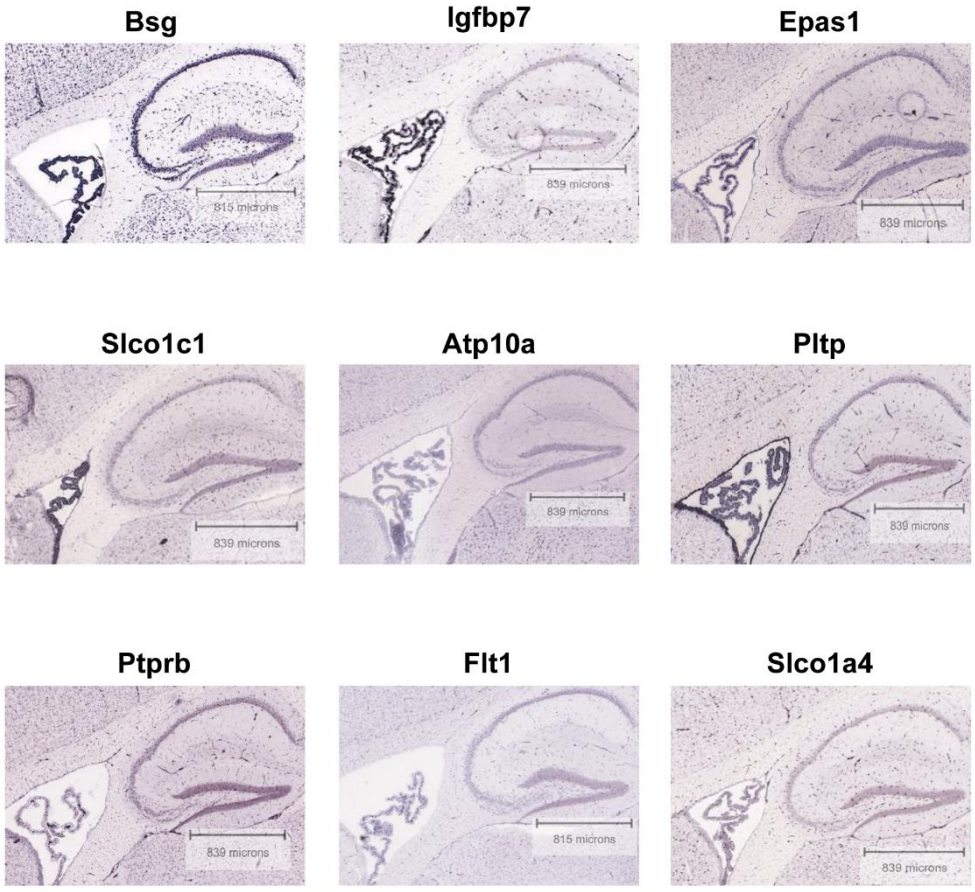

Supplemental Figure 9. Validation of endothelial cell-specific marker genes

The top marker genes for endothelial cells identified by our single cell sequencing approach were validated using the in-situ hybridization images in the Allen Brain Atlas (https://mouse.brain-map.org).

Supplemental Figure 10.

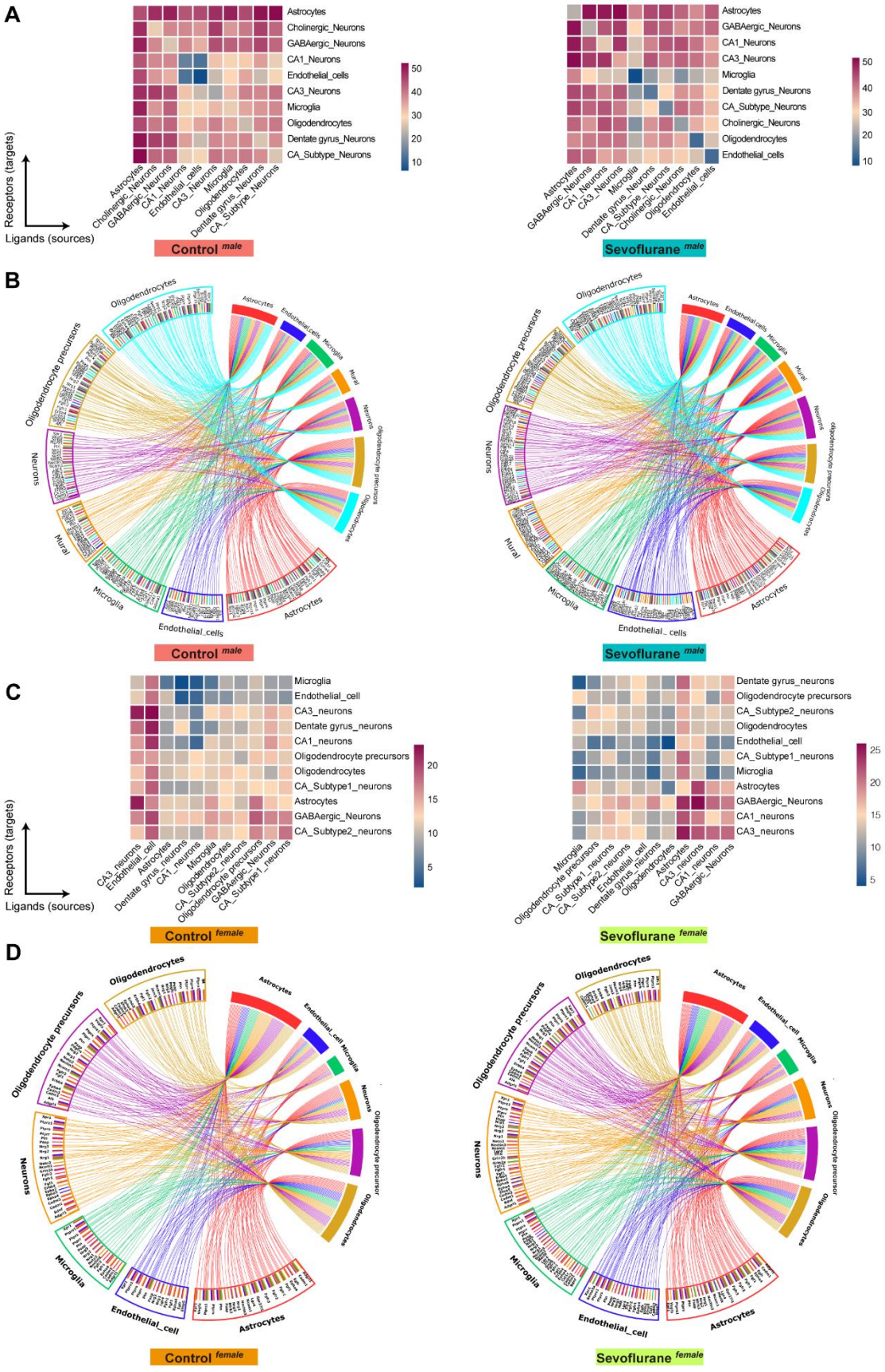

Supplemental Figure 10. Alterations in hippocampal cellular cross-talk induced by sevoflurane exposures in male and female mice

(A) Heatmaps showing the abundance of ligand-receptor interactions among source cells (columns) and target cells (rows) of hippocampus in the control ^{male} group (left) and sevoflurane ^{male} group (right). Darker purple indicates stronger interactions. **(B)** Circos plots showing significant cell-cell gene co-expression among source hippocampal cell types with secreted peptides (bottom half of the circus) and target cell types (top half of the circus) in the control ^{male} group (left) and sevoflurane ^{male} group (right). **(C)** Heatmaps showing the abundance of ligand-receptor interactions among source cells (columns) and target cells (rows) of hippocampus in the control ^{female} group (left) and sevoflurane ^{female} group (right). Darker purple indicates stronger interactions. **(D)** Circos plots showing significant cell-cell gene co-expression among source hippocampal cell types with secreted peptides (bottom half of the circus) and target cell types (top half of the circus) in the control ^{female} group (left) and sevoflurane ^{female} group (right). Criteria for significant enriched ligand-receptor pair: mincell_pct $\geq$ 30% and P value < 0.05 (CellPhoneDB software).

Supplemental Figure 11.

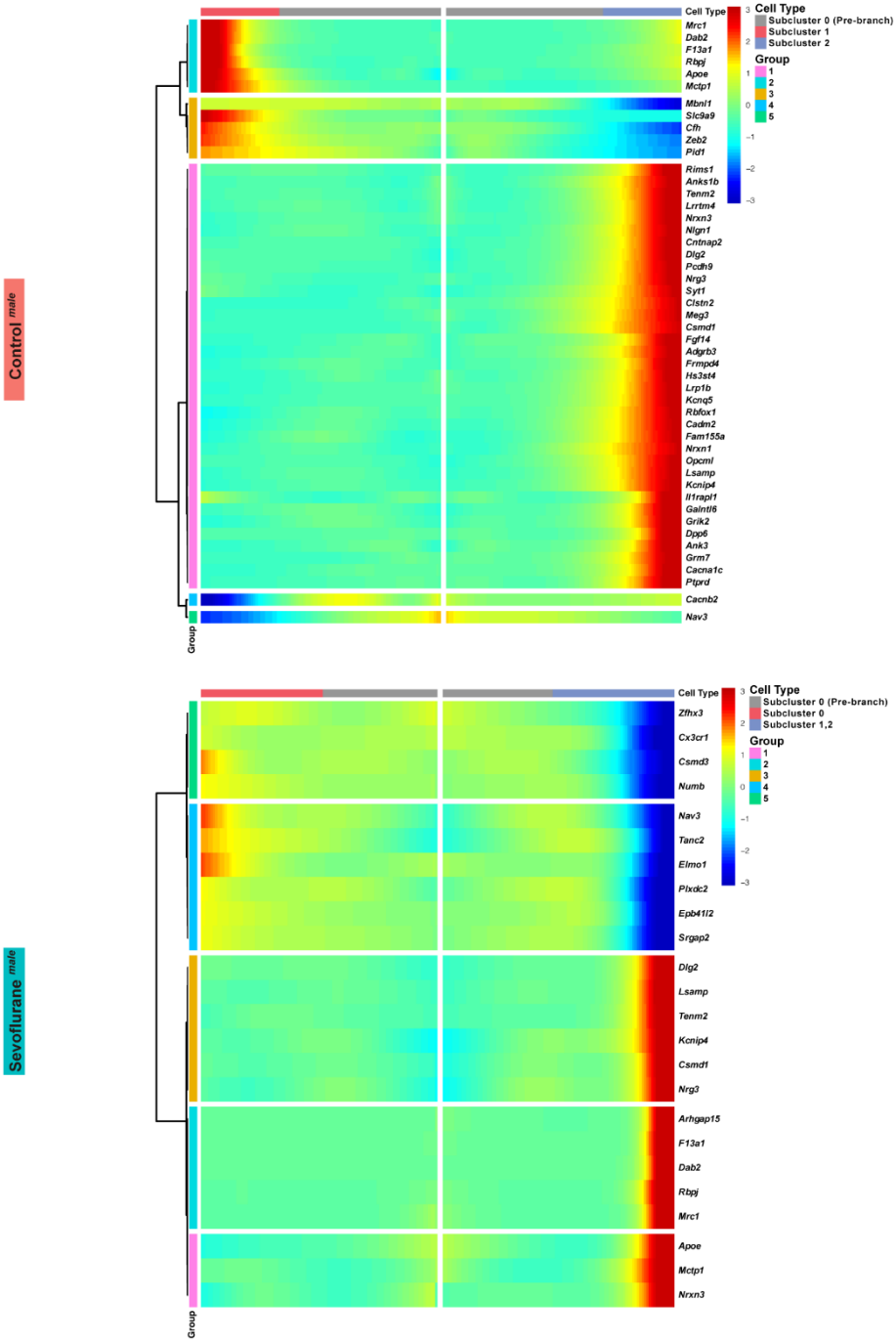

Supplemental Figure 11. Key genes that determined the differentiation branches of microglia in male mice

Heatmaps showing that the differential expression of key genes among subclusters 0, 1, and 2 determined microglia differentiation branches in the control ^{male} group (upper) and sevoflurane ^{male} group (lower). Criteria for key genes: false discovery rate < 1e-7 (Monocle 2 package).

Supplemental Figure 12.

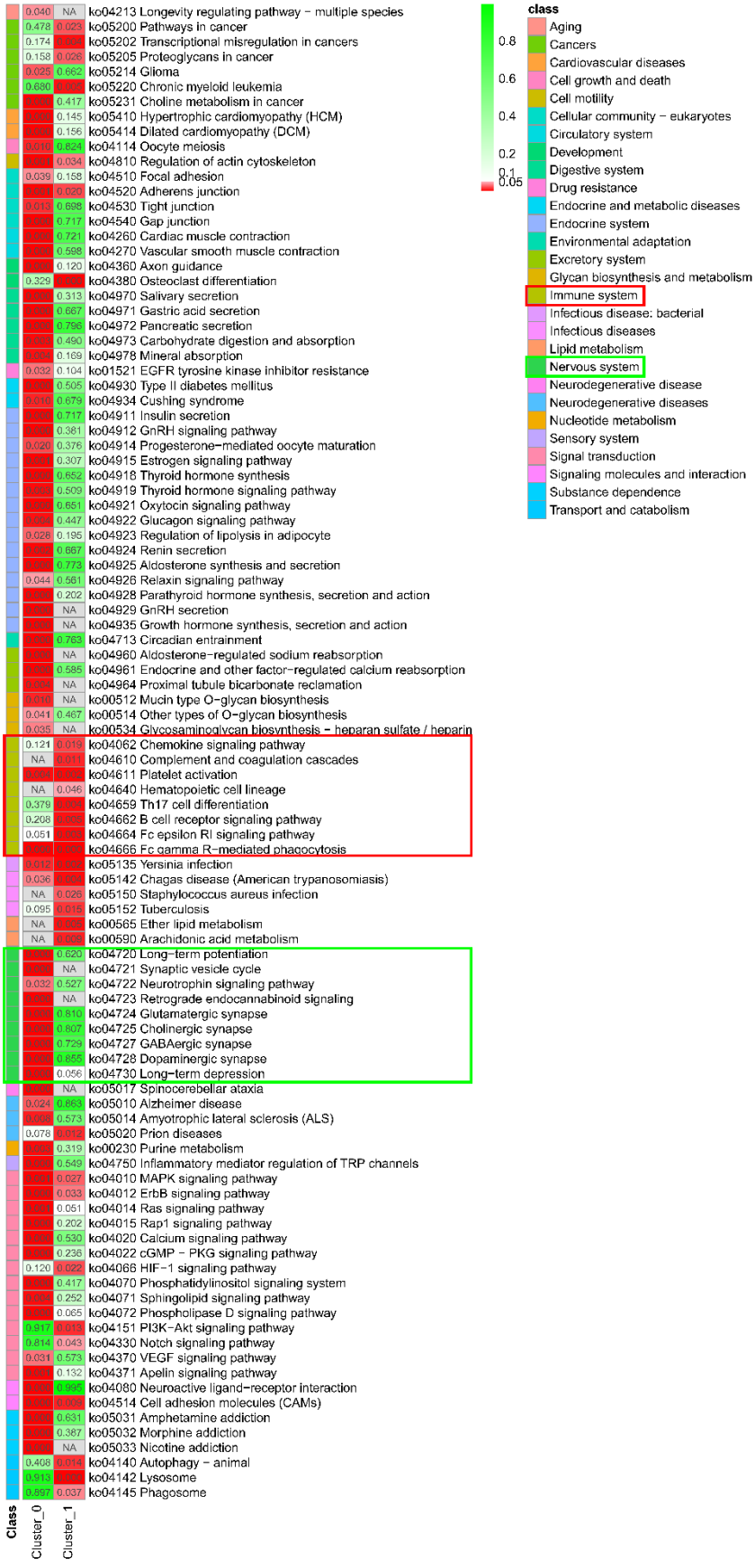

Supplemental Figure 12. Kyoto Encyclopedia of Genes and Genomes pathway enrichment analysis of microglia subclusters of female mice

Significantly enriched Kyoto Encyclopedia of Genes and Genomes pathways for subcluster 0 and 1 in relation to the nervous system and immune system, respectively. False discovery rate ≤ 0.05 as a threshold to determine a significant enrichment.

Supplemental Figure 13.

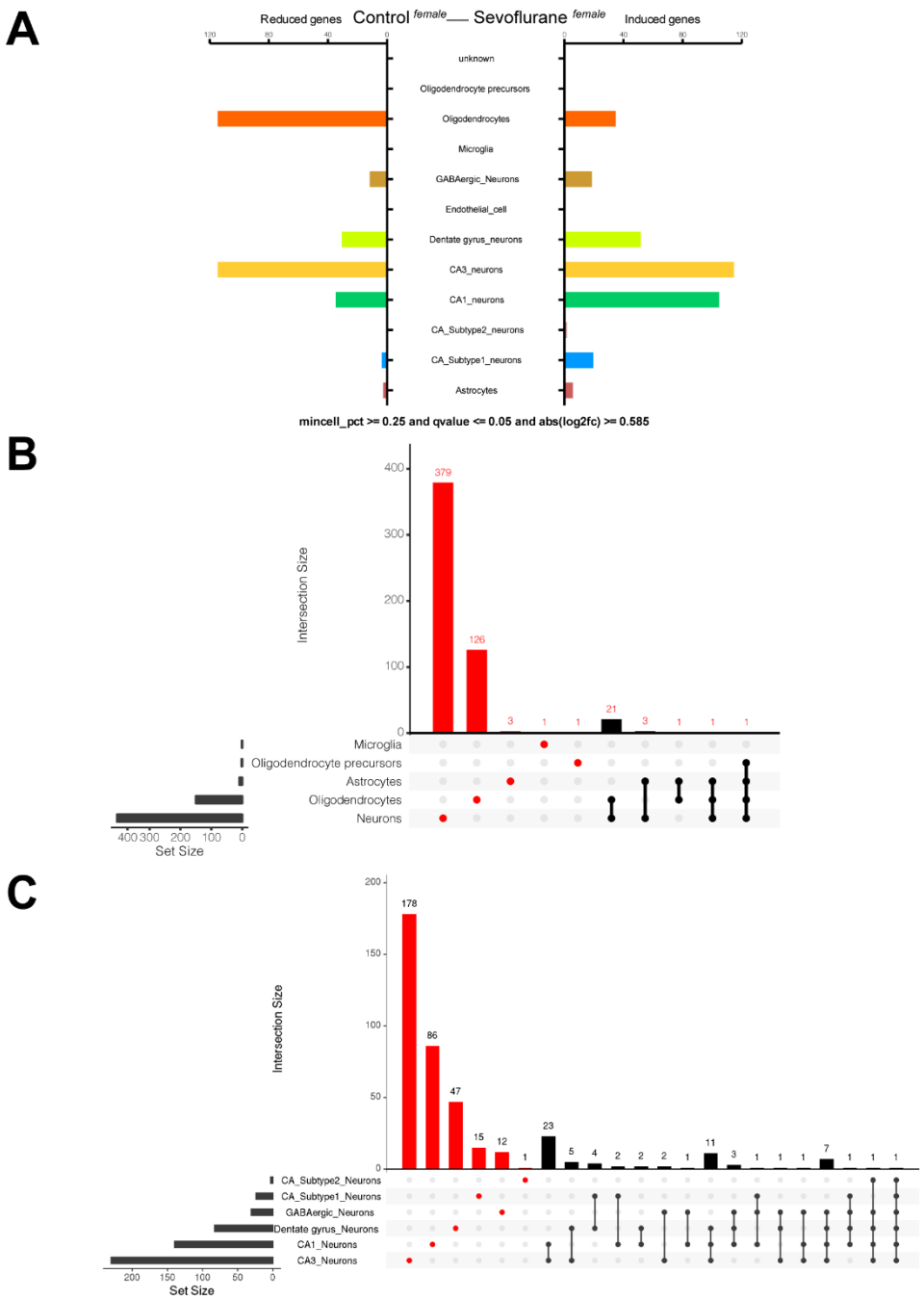

Supplemental Figure 13. Differentially expressed genes induced by sevoflurane exposures in hippocampal cell types in female mice

(A) Histogram showing the number of differentially expressed genes in each hippocampal cell type. **(B)** Histogram showing the number of differentially expressed genes in hippocampal cell types, with plots (red) indicating differentially expressed genes unique to a cell type and plots and lines (black) indicating common differentially expressed genes between ≥ 2 cell types. **(C)** Histogram with plots and lines showing the unique and common differentially expressed genes in hippocampal neuron subtypes. Criteria for differentially expressed genes: mincell_pct ≥ 0.25, q value ≤ 0.05, and $|\log_2$ (fold change) $| \geq 0.585$ (Model-based Analysis of Single-cell Transcriptomics test).

Supplemental Figure 14.

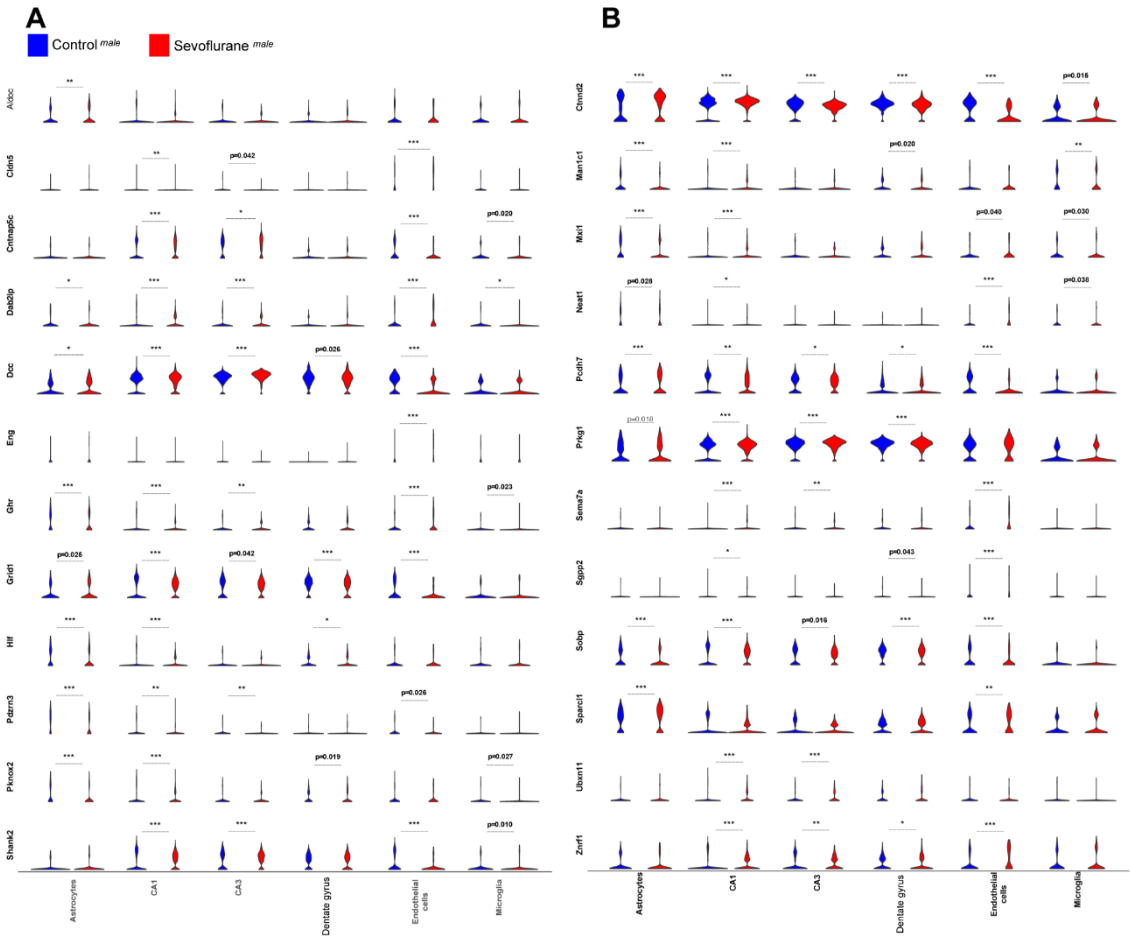

Supplemental Figure 14. Normalized expression of common differentially expressed genes in specific hippocampal cell types in male mice

Violin plots showing the normalized expression of 24 common differentially expressed genes in specific hippocampal cell types in the control ^{male} group (blue) and sevoflurane ^{male} group (red). Data are means ± SD. n = 15–3154 cells/group. Student's t-test. *P < 0.02, **P < 0.01, ***P < 0.001.

Supplemental Figure 15.

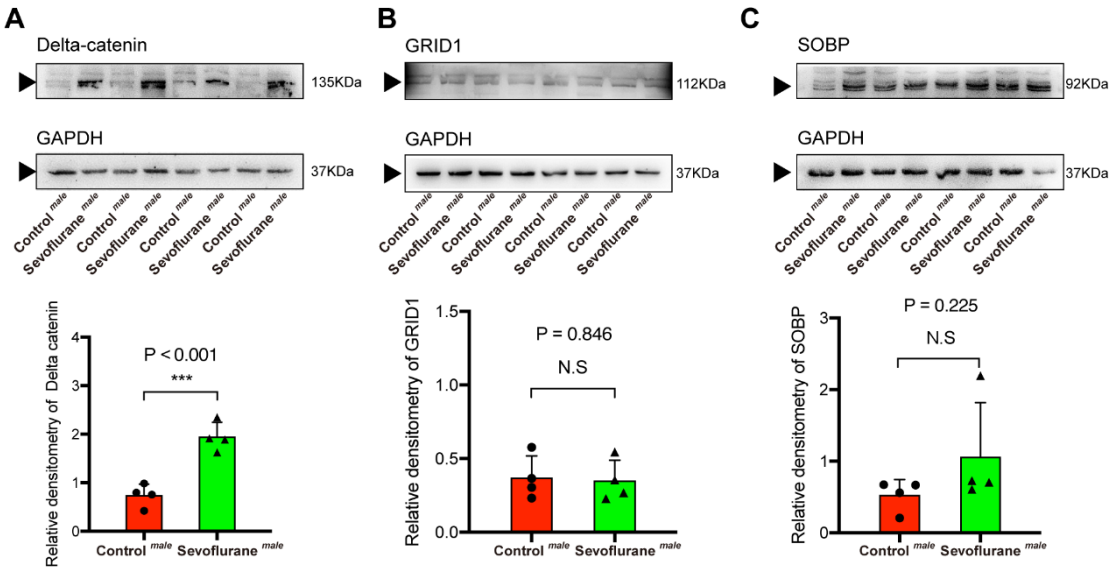

Supplemental Figure 15. Protein expression of delta-catenin, GRID1, and SOBP in male mice using Western blot

(A) Protein bands and expression analysis showing that the sevoflurane ^{male} group had upregulated expression of delta-catenin (mean difference = 1.20, 95%CI: 0.74 to 1.67, P < 0.001). **(B, C)** Protein bands and expression analysis showing that the expression of GRID1 and SOBP was comparable between groups. Data are means ± SD. n = 4 mice/group. Student's t-test.